ISTITUTO NAZIONALE DI FISICA NUCLEARE

Sezione di Catania

INFN/TC-88/15
20 Aprile 1988

F. Bonomo, J. Romanski, C. Tuvé, R. Barnà and D. De Pasquale:

TRANSPARENT ΔE GAS DETECTOR FOR HEAVY IONS.

Servizio Documentazione
dei Laboratori Nazionali di Frascati

INFN - ISTITUTO NAZIONALE DI FISICA NUCLEARE
Sezione di Catania

F.Bonomo, J.Romanski, C.Tuvé, R.Barnà, D.De Pasquale

TRANSPARENT ΔE GAS DETECTOR FOR HEAVY IONS

TRANSPARENT ΔE GAS DETECTOR FOR HEAVY IONS

F.Bonomo, J.Romanski*, C.Tuvé
Dipartimento di Fisica, Università di Catania, Italy
Istituto Nazionale di Fisica Nucleare, Sezione di Catania, Italy

R.Barnà, D.De Pasquale
Istituto di Fisica, Università di Messina, Italy
Istituto Nazionale di Fisica Nucleare, Sezione di Catania, Italy

ABSTRACT

A small, 50×60×50 mm^3 gas chamber was realized to be used as transparent ΔE detector in front of solid state position sensitive detectors (PSD). It has two rectangular openings, covered by thin polypropylene foils (t≃1000 Å). The electrical field is along the particle trajectory, with electron collection at the centre of the chamber. Tests by ^{12}C ions of $E_{lab} \simeq 54$ MeV, done using the chamber in telescope with a silicon PSD, have shown its good linearity and energy resolution.

1. - INTRODUCTION

The telescopes of detectors are the most used tools to identify particles produced in heavy ion reactions. However, when the energy of the particles is not sufficiently large, it is difficult to use solid detectors as ΔE detectors, for they must be extremely thin. It is better, in many cases, to use gas detectors for ΔE measurements.

Ionization chambers (IC) to detect heavy ions have been extensively studied, built and used[1-10], so that the principles of their functioning are well known. Many of them use a solid state detector placed inside[5-8]. However, when one prefers to use PSD's, this configuration is perhaps not the best, since in some runs during measurements, one must put in front of the PSD a grid, that is a system of parallel slits, to calibrate the 'position' signals of the detector[11,12]. It is useful to put the grid at small distances from the detector and, if possible, without matter between them, to avoid angular spread out of the impinging ions. So we chose to

* on leave of absence from the Physics Institute of the Jagellonian University, Krakow, Poland.

build a chamber with two windows, both covered by thin foils, to use it as transparent ΔE detector, put outside the PSD.

Some of the chambers have the electric field perpendicular to the particle trajectory[3-5,7-9]: this allows to put a Frisch grid inside the chamber to improve the electron collection. We preferred, on the contrary, following the suggestion of a C.R.N.S. group[6], to use a longitudinal electric field. This allows to maintain small the dimensions of the chamber having at the same time all the walls at ground potential without distorting the internal field. This smallness of the chamber is very useful if one needs to do measurements at very small angles ($\theta \simeq 0^{o}$).

Different gases and mixtures of gases have been studied and used[13,14] and one knows their transport properties for electrons and ions. We have studied the Ar-CH_4 mixture and isobutane, because of their good production of electric signals. We have chosen isobutane, which produces signals rather insensitive to the electric field inside the chamber[13,15].

The description of the ionization chamber (IC) and the results we have obtained in the calibration by ^{12}C ions accelerated by the MP Tandem of the National Laboratories of Southern Italy (LNS) in Catania are in sect. **2**; the conclusions are in sect. 3.

2. - THE TRANSPARENT ΔE IONIZATION CHAMBER

2.1. - Description of the chamber

Fig.1 reports the photography of the chamber, closed (fig.1a) and open (fig.1b). As one can see, it is formed by an almost cubic container inside which six rectangular, parallel and equally spaced rings are put. The third ring starting from the end is at $V_{max}>0$; it has the inner opening slightly smaller than the other rings and is constitued by two rings, one inside the other and connected by a resistance. The outer ring brings the HV, the inner one is the collection ring and is connected to the preamplifier.

The electrical scheme of the chamber is shown in fig. 2. As one can see, the distribution of potential is asymmetric with respect to the centre of the chamber: this is useful to compensate, at least partially, the component of the electron speed along the particle trajectory.

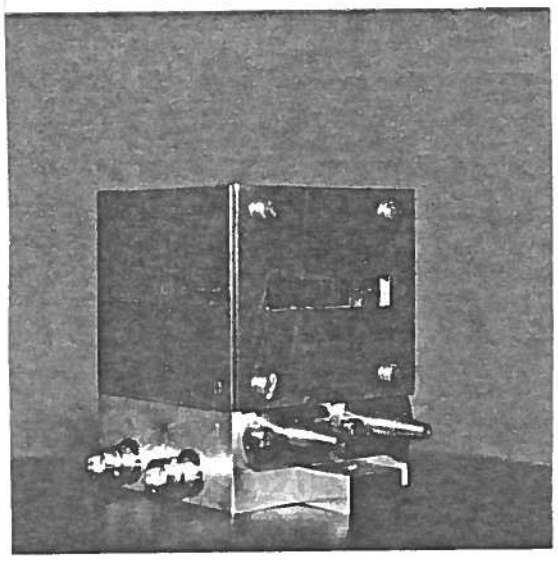

Fig. 1a

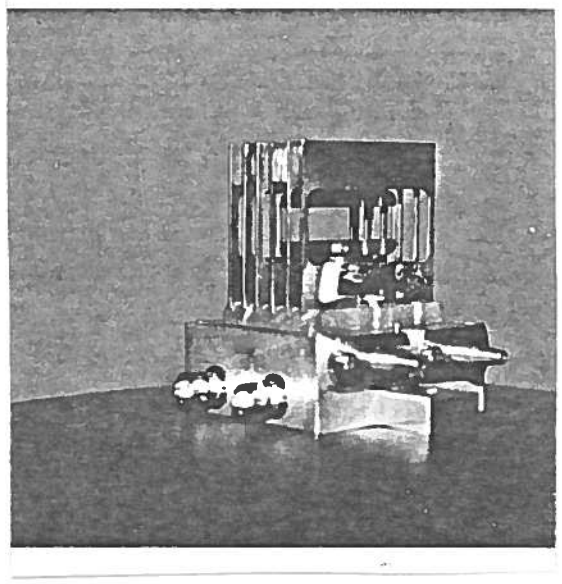

Fig. 1b

Fig. 1 - The ionization chamber: a) closed chamber; b) open chamber showing the configuration of the potential rings.

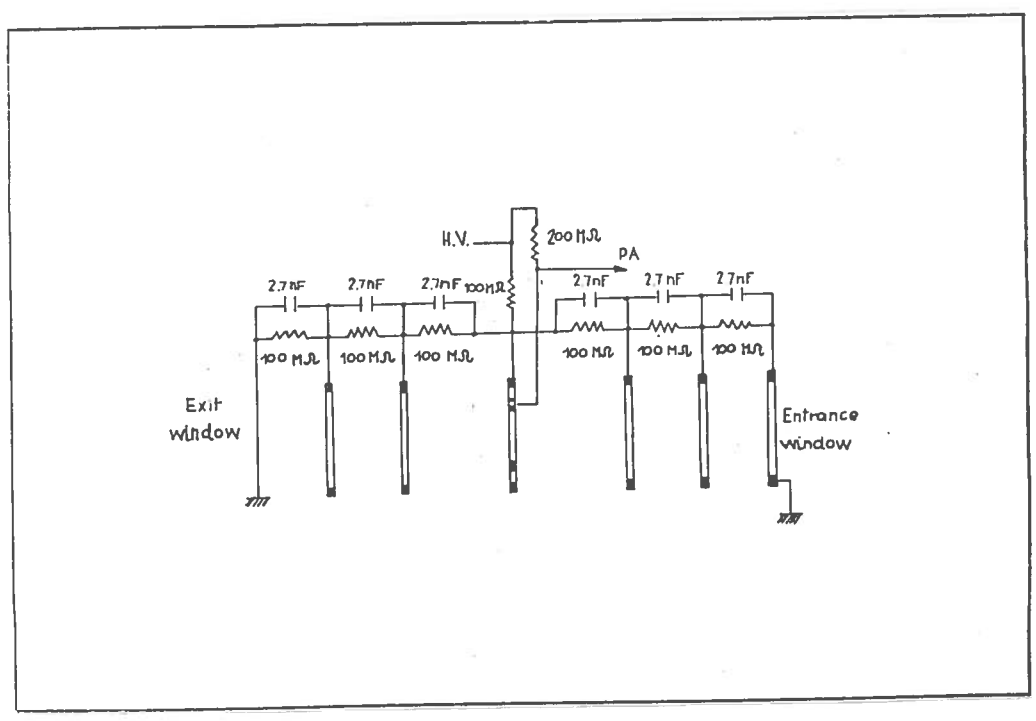

Fig. 2

Fig. 2 - Electrical scheme of the ionization chamber.

The two parallel rectangular openings, 50×6 mm^2, centered on the chamber axis, which appear on the front and rear walls of the chamber, are covered by ≈1000 Å thin polypropylene foils glued on the inner sides of the metallic walls and supported by the pressure

rings. The thickness of the foils and their uniformity were optically controlled[16]. So it was possible to correct well for dead paths of the particles in the chamber.

2.2 - Calibration of the chamber: experimental procedure.

The ionization chamber was filled by isobutane in the continuous gas flow system schematically reported in fig. 3. The pulses produced in the chamber were sent to a PC-series ORTEC preamplifier, then to the main amplifier and finally recorded by the acquisition system.

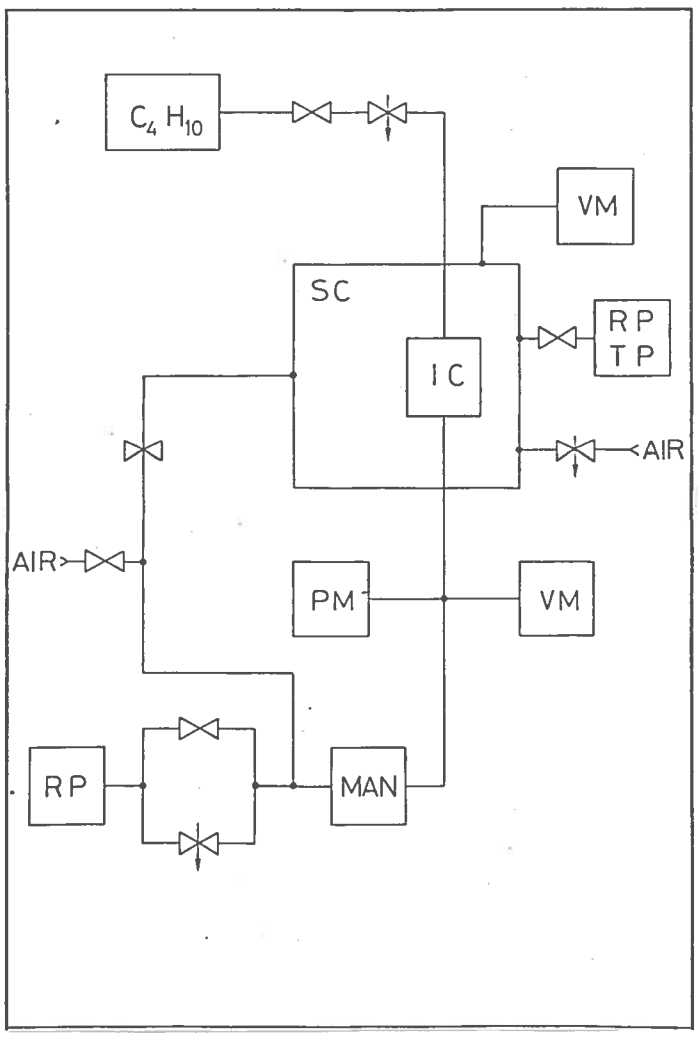

Fig. 3

Fig. 3 - Schematical representation of the gas flow system: C_4H_{10} = gas bomb, SC = scattering chamber, IC = ionization chamber, RP = rotary pump, TP = turbomolecular pump, PM = absolute pressure meter, VM = vacuum gauge, MAN = membrane manostat.

The pressure was stabilized by a membrane manostat supplied by Leybold-Heraeus Co., having a stability of 1%. Two different gas

pressures (50 mbar and 100 mbar) and two different values of the HV (V_{max}=250 V and V_{max}=500 V) were used in a first test of the chamber by a three peaks ^{239}Pu-^{241}Am-^{243}Cm α-source, with α-particles energies of 5.15, 5.48 and 5.79 MeV, respectively. The pulse heigths were well proportional to the pressure, but showed to depend a little on the HV values: this means that it is difficult to reach the saturation in the charge collection with the chosen configuration of the electric field.

From the results of the test the values of p=100 mbar and V_{max}= 500 V were chosen to work with heavy ions.

The IC was put inside the scattering chamber of the LNS, and mounted on one of the rotating platforms. A silicon PSD, supplied by ENERTEC, 300 μm thick, screened by a 45×6 mm^2 diaphragm, was placed behind the rear window at a distance of 2 cm, sufficient to allow a calibration grid, rotating independently with the other platform, to be inserted between the chamber and the detector. The distance of the detector from the target was ≃33.6 cm, so that it covered an angular range of 7.6^{o}.

The target was self supporting enriched ^{11}B≃100 $\mu g/cm^2$ thick. A ^{12}C beam, with an intensity of ≃2 pnA, accelerated to E=56 MeV from the 15 MV Tandem of the LNS, was sent on the target.

The central angle of the telescope was fixed at 10.3^{o}. So, during the experiment, the scattered ^{12}C particles were detected between 6.5^{o} and 14.1^{o}. The most part of them were, of course, elastically scattered, so that the energies varied between 55.0 MeV and 52.7 MeV. The angle calibration of the PSD was done placing in front of it a grid, constitued by ten parallel slits, 0.3 mm wide, orthogonal to the detector axis, grouped five by five. The distance between the centres of two adiacent slits in each group was 3.1 mm, while the two nearest ones of both groups were distant 6.2 mm. So the system appeared as one of 11 slits, with the central one missing: this is very useful to check well the position of the central angle when analysing the data.

The pulses produced in the PSD and those produced un the IC were amplified, digitalized and sent in coincidence to the acquisition system. The experimental set up is schematically represented in fig. 4.

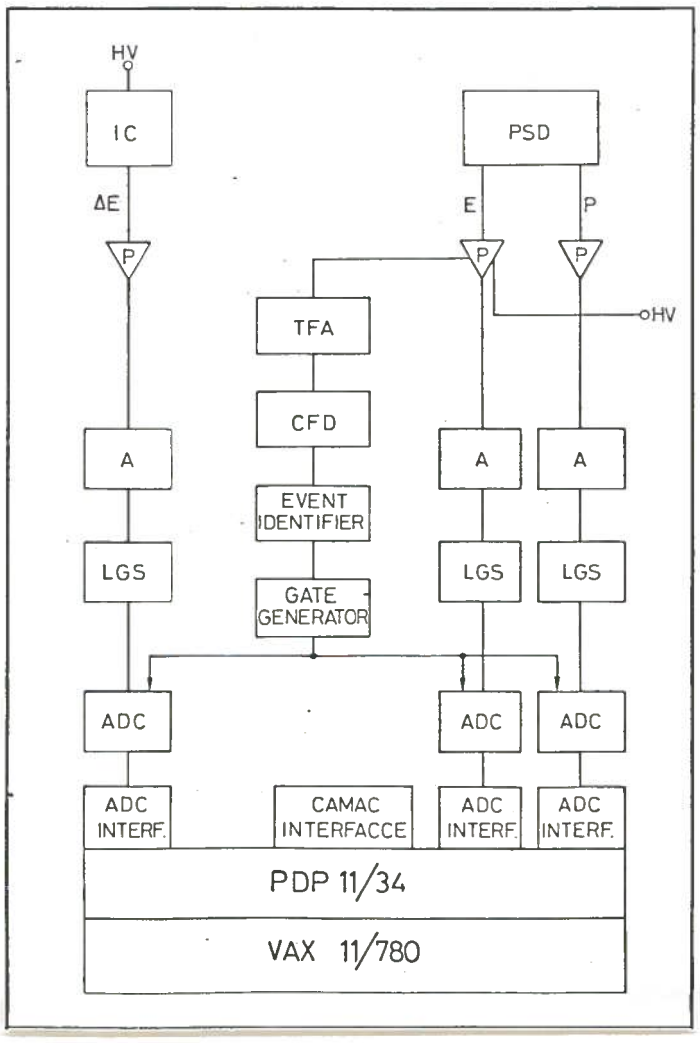

Fig. 4.

Fig. 4 - Experimental set up of the chamber-PSD telescope

2.3. - Calibration of the chamber: results.

Using the 'energy' and 'position' pulses given by the PSD when the grid was in front of it, the angular calibration of the telescope was obtained.

Fig. 5 shows the bidimensional linearized pulse heigth spectrum of the telescope, when the calibration grid was removed. The different paths in the gas of the particles having different angles of incidence on the entrance window are taken into account by the factor $1/\cos(\theta-\theta_o)$ in their energy loss, being θ_o the angle of emission of the particles at the centre of the window.

Choosing then the pulses produced by the elastically and inelastically scattered ^{12}C ions, it was easy to compute the energy loss ΔE associated to the heigth of each pulse from the IC and to calib-

rate it. The values of the specific energy losses dE/dx were obtained by the well known tables of J.F.Ziegler [17].

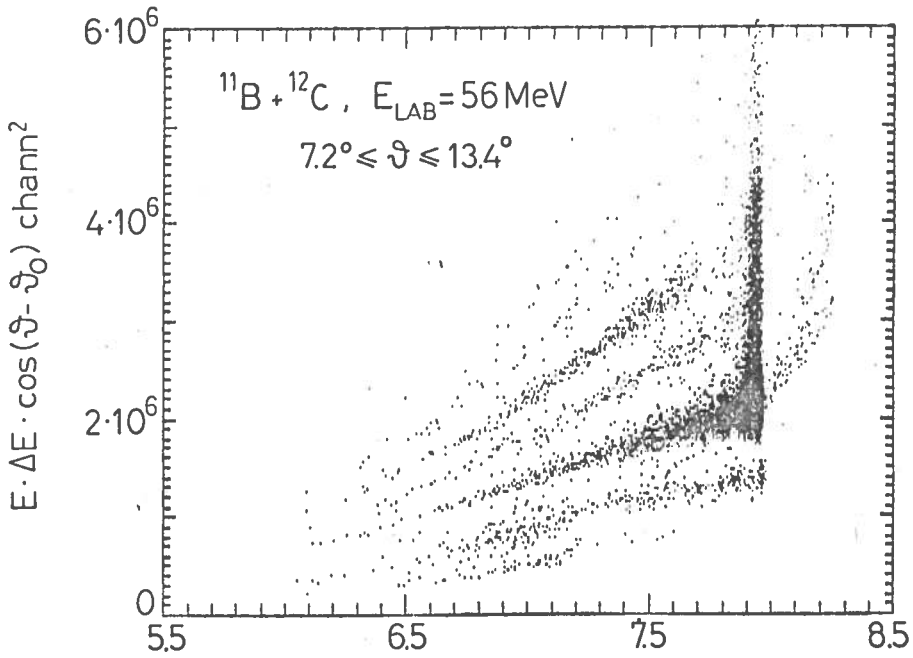

Fig. 5.

Fig.5 - Linearized bidimensional spectrum of the telescope pulses. E and ΔE are the channel numbers of the 'energy' pulses of the PSD and of the IC, respectively. When the energy loss is much smaller than the energy and this last is sufficiently high to avoid charge variations of the incident ion, one must obtain $\Delta E \cdot E/\Delta s \simeq a(Z,M) + b(Z,M) \cdot \ln E$, due to the linearity of the used detectors, with $\Delta s \simeq 1/\cos(\theta-\theta_0)$.

The energy response of the chamber is shown in fig. 6. The energy resolution is ≃ 6%, which corresponds to a resolution of ≃ 3% in Z and M, as one can extimate in part also from fig. 5 and from fig. 7, where the bidimensional spectrum of $Z\sqrt{M}$ vs E is shown for the particles produced in the used heavy ion collision. This energy resolution is measured relatively to Z=6, due to much higher number of pulses of carbon ions.

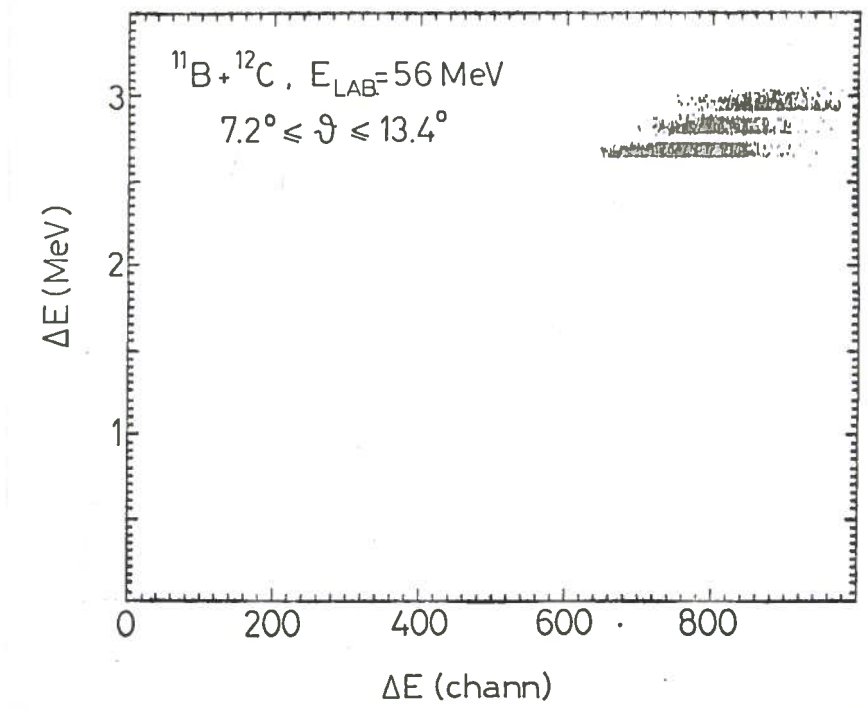

Fig. 6.

Fig. 6 - Energy calibration of the ionization chamber by ^{12}C nuclei scattered elastically and inelastically by ^{11}B at E_{inc}=56 MeV

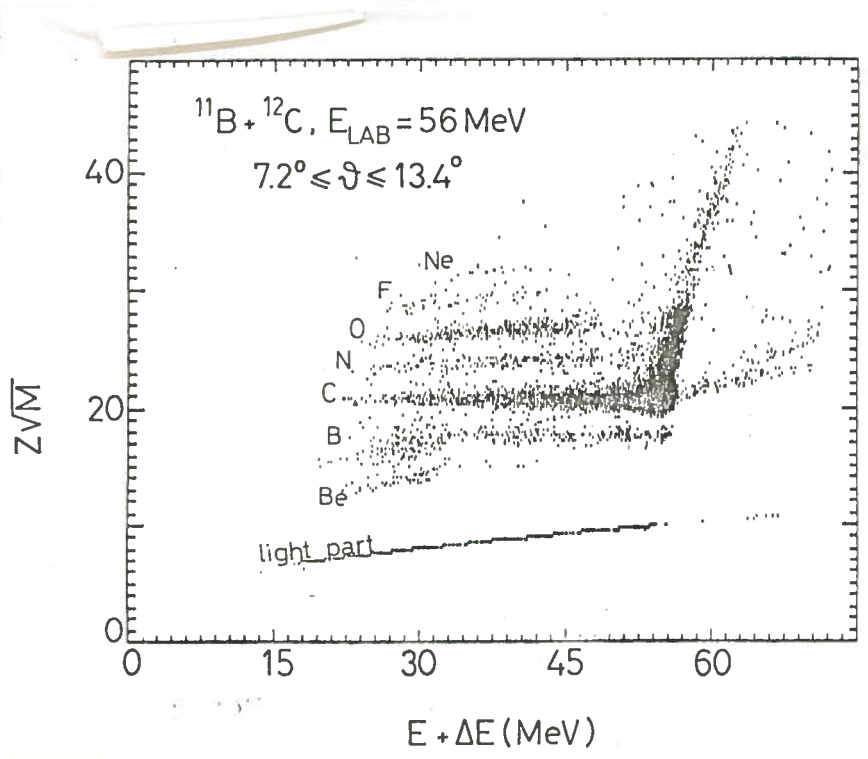

Fig. 7.

Fig. 7 - Bidimensional spectrum $Z\sqrt{M}=\sqrt{\{ E \cdot \Delta E \cos(\theta-\theta_0)/[a'+b'\ln(E/M)]\}}$ vs E+ΔE. All the pulses result distributed on horizontal straight lines placed at the different $Z\sqrt{M}$ values. Here E and ΔE are the true values of the energy and energy loss of the particles, as measured by the PSD and the IC, respectively.

3. - CONCLUSIONS

The ionization chamber we have realized for charge identification of heavy ions is particularly suitable to be used in connection with solid state PSD's, due to its configuration as transparent gas detector.

Used with isobutane gas at moderately low pressures it gives a pulse width of 130 keV for α-particles loosing 2 MeV inside it and 160 keV for ^{12}C particles loosing 2.7 MeV. This width seems to be independent on the energy loss and on the HV supply.

The smallness of the chamber makes it very useful when measurements at very forward angles are required.

ACKNOWLEDGEMENTS :

The authors would like to acknowledge Prof's. V.D'Amico, R.Potenza and A.Strazzeri for the encouragement to begin the work and the many useful discussions during it. Thanks are also due to Mr. G.Poli for his assistance and his useful advices for the technical realizations and to Mr. M.Mazzeo and the staff of the workshop of the Physics Dept. of Catania for the care in realizing the different parts of the ionization chamber.

REFERENCES :

1) H.W.Fulbright - Nucl. Instr. Meth. 162 (1979) 21

2) A.Oed, P.Geltenbort and F.Goennenwein - Nucl. Instr. Meth. 205 (1983) 451

3) U.Quade, K.Rudolph and G.Siegert - Nucl. Instr. Meth. 164 (1979) 435

4) Z.Sosin, T.Kozik, S.Micek and K.Grotowski - Nucl. Instr. Meth. A249 (1986) 344

5) R.G.Stockstad, D.C.Hensley and A.Snell - Nucl. Instr. Meth. 141 (1977) 499

6) J.C.Adloff, D.Disdier, V.Rauch and F.Scheibling - C.R.N.S. Rapport d'attivité 1979 - C.R.N. 80-01, p.61, Strasbourg 1980

7) T.R.Ophel, W.Galster, D.J.Hinde and J.R.Leigh - Nucl. Instr. Meth. 193 (1982) 507

8) R.W.Zurmuhle and L.Csihas - Nucl. Instr. Meth. 203 (1982) 261

9) G.Prete, D.Fabris, G.Fortuna, F.Gramegna, M.Morando and A.Viesti - Nucl. Instr. Meth. 195 (1982) 617

10) C.P.M. Van Engelen, R.Jelmersma, A. Van den Brink and R.Kamermans - Nucl. Instr. Meth. 228 (1984) 69

11) H.Emling, R.Novotny, D.Pelte and G.Schrieder - Nucl. Phys. A211 (1973) 600

12) B.Bilwes, R.Bilwes, V.D'Amico, J.L.Ferrero, G.Giardina and R.Potenza - Nucl. Phys. A408 (1983) 173

13) G.Shultz and J.Gresser - Nucl. Instr. Meth. 151 (1978) 413

14) L.G.Cristophorou, D.L. McCorkle, D.V.Maxey and J.G.Carter - Nucl. Instr. Meth. 163 (1979) 141

15) V.Palladino and B.Sadoulet - Nucl. Instr. Meth. 128 (1975) 323

16) F.Porto and S.Sambataro - private communication

17) J.F.Ziegler (ed.) - The stopping and ranges of ions in matter - Pergamon Press - New York, 1977